2108 *Organometallics* **1996,** *15,* 2108−2117

Synthesis and Characterization of Group 14−Platinum(IV) Complexes

Christopher J. Levy, Jagadese J. Vittal, and Richard J. Puddephatt*

Department of Chemistry, The University of Western Ontario,
London, Ontario, Canada N6A 5B7

Received June 26, 1995[⊗]

The reactions of group 14 compounds Me_nEX_{4-n} (E = Si, Ge, Sn; X = Cl, Br, I) with electron-rich [$PtMe_2$(diimine)] complexes give facile *trans* oxidative addition of the E−X bond (E = Si, X = Br, I; E = Ge, Sn, X = Cl, Br, I). The oxidative additions occur more readily for Me_nEX_{4-n} in the sequences X = I > Br > Cl and E = Sn > Ge > Si. The first stable silylplatinum(IV) complexes have been prepared in this way, and the X-ray crystal structure of [$PtIMe_2(Me_3Si)$(bpy)] shows an exceptionally long Pt−I bond length (2.963(1) Å) consistent with the high *trans* influence of the trimethylsilyl group. ^{1}H NMR studies show that the oxidative addition involving germanium and tin reagents is easily reversible. Several of the platinum(IV)−tin complexes have a second molecule of tin reagent incorporated into the crystal lattice. The X-ray crystal structure of [$PtIMe_2(Me_3Sn)$(bpy-^{t}bu$_2$)]$_2$·Me_3SnI·CH_2Cl_2 shows two distinct complexes (1:1 ratio) to be present in the unit cell. The first is the product of *trans* oxidative addition, [$PtIMe_2(Me_3Sn)$(bpy-^{t}bu$_2$)], and the second is [$PtIMe_2(Me_3Sn)$(bpy−^{t}bu$_2$)]·Me_3SnI. In this second complex the platinum-bound iodo ligand coordinates to the tin center of the Me_3SnI molecule to give a trigonal-bipyramidal tin center.

Introduction

There is an emerging greater use of group 14−transition metal species in the catalysis of organic transformations. Several group 14−platinum systems have been found to be catalytic, and the reactions are believed to involve platinum(IV) complexes as intermediates. Silylplatinum(IV) intermediates are generally proposed in the hexachloroplatinic acid-catalyzed hydrosilylation of alkenes.[1,2] Platinum-catalyzed hydrogermylation is similarly believed to proceed *via* germylplatinum(IV) intermediates.[3] Platinum(IV)−tin intermediates are proposed for the Pt/Sn/Cl-catalyzed hydrogenation and hydroformylation of alkenes,[4,5] as well as for the platinum−tin-catalyzed water gas shift reaction.[6] Despite the importance of group 14−platinum(IV) complexes in catalytic cycles, relatively few have been isolated. Ebsworth and co-workers[7,8] have reported the only known silylplatinum(IV) complexes, although these were not stable and were only characterized spectroscopically. Similarly, very few platinum(IV)−tin and −germanium complexes have been isolated.

There has been little study of the oxidative addition of group 14−halide bonds to platinum(II) except when the group 14 element is carbon. In one notable study, Kuyper[9,10] describe the oxidative addition of compounds ER_nCl_{4-n} (E = Sn, Ge; R = Me, Ph) to [$PtMe_2$(bpy)]. The oxidative addition of silicon−chloride bonds was attempted but never observed. Herein we describe the oxidative addition of Me_3EX (E = Ge, Sn; X = Cl, Br, I) to a number of platinum(II) complexes. Furthermore we report the first examples of stable platinum(IV) products resulting from silicon−halide oxidative additions to platinum(II) centers. A preliminary account of part of this work has been published.[11]

Chart 1. Structures of Diimine Ligands with Labeling Systems

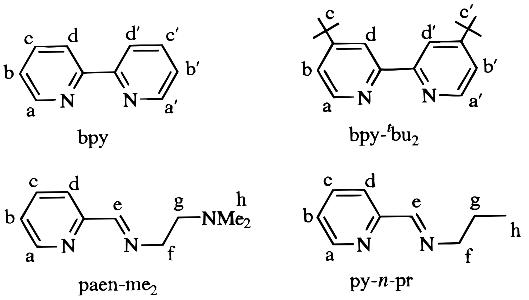

Results and Discussion

Synthesis of New Complexes. Four diimine ligands were employed in this work (Chart 1). Bipyridine (bpy) has great utility as an electron-donating ligand which facilitates oxidative addition reactions to transition metal centers. 4,4′-Di-*tert*-butyl-2,2′-bipyridyl (bpy-^{t}bu$_2$) offers similar ligating properties to bpy but offers

---

[⊗] Abstract published in *Advance ACS Abstracts,* April 1, 1996.

(1) Cundy, C. S.; Kingston, B. M.; Lappert, M. F. *Adv. Organomet. Chem.* **1973**, *11*, 253.

(2) Pawlenko, S. *Organosilicon Chemistry*; Walter de Gruyter: New York, 1986; p 36.

(3) Fish, R. H.; Kuivila, H. G. *J. Org. Chem.* **1966**, *31*, 2445.

(4) Hartley, F. R. *Chemistry of Platinum and Palladium: Recent Developments*; Elsevier: New York, 1991; pp 384, 385.

(5) McKay, K. M.; Nicholson, B. K. In *Comprehensive Organometallic Chemistry*; Wilkinson, G., Stone, F. G. A., Abel, E. W., Eds.; Pergamon: Oxford, 1982; Vol. 6.

(6) Kubota, M. *Inorg. Chem.* **1990**, *29*, 574.

(7) (a) Bentham, J. E.; Ebsworth, E. A. V. *Inorg. Nucl. Lett.* **1970**, *6*, 145. (b) Bentham, J. E.; Cradcock, B. S.; Ebsworth, E. A. V. *J. Chem. Soc. A* **1971**, 587.

(8) Anderson, D. W. W.; Ebsworth, E. A. V.; MacDougall, J. K.; Rankin, D. W. H. *J. Inorg. Nucl. Chem.* **1973**, *35*, 2259.

(9) Kuyper, J. *Inorg. Chem.* **1977**, *16*, 2171.

(10) Kuyper, J. *Inorg. Chem.* **1978**, *17*, 77.

(11) Levy, C. J.; Puddephatt, R. J.; Vittal, J. J. *Organometallics* **1994**, *13*, 1559.

0276-7333/96/2315-2108$12.00/0

Scheme 1

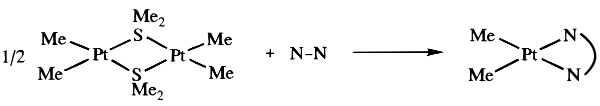

1-4

1, N-N = bpy; **2**, N-N = bpy-^{t}bu$_2$; **3**, N-N = py-*n*-pr; **4**, N-N = paen-me$_2$

Scheme 2

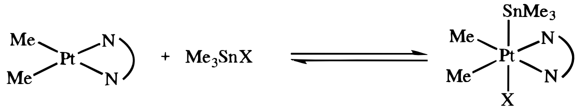

7a-d, 8a-c, 9a-c

7a, N-N = bpy, X = Cl; **7b**, N-N = bpy-^{t}bu$_2$, X = Cl; **7c**, N-N = py-*n*-pr, X = Cl; **7d**, N-N = paen-me$_2$, X = Cl; **8a**, N-N = bpy, X = Br; **8b**, N-N = py-*n*-pr, X = Br; **8c**, N-N = paen-me$_2$, X = Br; **9a**, N-N = bpy, X = I; **9b**, N-N = py-*n*-pr, X = I; **9c**, N-N = paen-me$_2$, X = I

Scheme 3

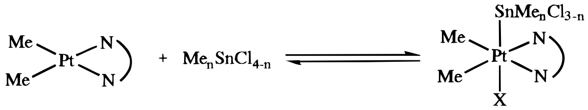

10a,b 11 12

10a, N-N = paen-me$_2$, n = 2; **10b**, N-N = bpy-^{t}bu$_2$, n = 2; **11**, N-N = paen-me$_2$, n = 1; **12**, N-N = paen-me$_2$, n = 0

Scheme 4

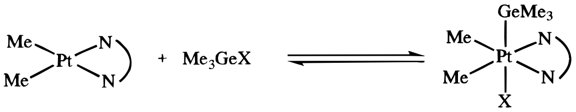

13-15

13, N-N = bpy-^{t}bu$_2$, X = Cl; **14**, N-N = bpy-^{t}bu$_2$, X = Br; **15**, N-N = bpy-^{t}bu$_2$, X = I

Scheme 5

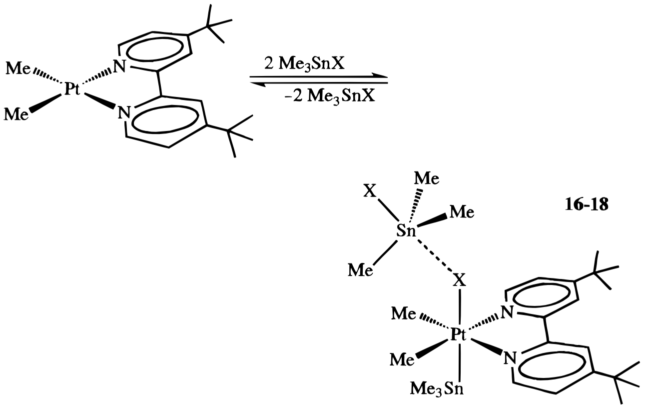

16-18

16, X = Cl; **17**, X = Br; **18**, X = I

improved solubility of metal complexes. The *N*-(*β*-*N*′,*N*′-dimethylaminoethyl)pyridinealdimine ligand (paen-me$_2$) possesses a dangling dimethylamino group which has the potential to coordinate to a group-14 element to afford a five-coordinate center. Furthermore, the dimethylamino group has the potential to coordinate weakly to the platinum center and so could provide anchimeric assistance for the oxidative addition reactions. As a control to determine if such effects do occur, the analogous ligand with a simple *n*-propyl side chain in place of the *N*,*N*-dimethylaminoethyl group was also prepared.

The [PtMe$_2$(diimine)] complexes were synthesized by the addition of the diimine ligands to suspensions of [Pt$_2$Me$_4$(*μ*-SMe$_2$)$_2$] (Scheme 1). The platinum(IV) complexes formed by oxidative addition to [PtMe$_2$(bpy-^{t}bu$_2$)] have a considerably higher solubility in common organic solvents compared to the products obtained from addition to [PtMe$_2$(bpy)]. Little difference was seen between the oxidative addition reactions of [PtMe$_2$(paen-me$_2$)] and [PtMe$_2$(py-*n*-pr)] indicating that any group 14−dangling nitrogen interactions are of little significance. Attempted oxidative additions of Me$_3$EI (E = Si, Sn) to [PtMeI(bpy-^{t}bu$_2$)] were unsuccessful, indicating that more electron-rich platinum centers, such as are found in the [PtMe$_2$(diimine)] complexes of this work, are required for the oxidative addition of group 14−halide bonds to occur.

The oxidative additions of Me$_3$GeCl, Me$_3$GeBr, and Me$_3$SnCl to [PtMe$_2$(bpy)] described here were first reported by Kuyper.[9,10] These reactions have been extended to the oxidative addition of a wide variety of germanium and tin reagents to platinum(II) complexes of the general formula [PtMe$_2$(diimine)] (Schemes 2−4). The oxidative additions of Ge−X and Sn−X (X = Cl, Br, I) to platinum(II) proceeded rapidly and cleanly to give the platinum(IV) products in good yield. The platinum(IV) complexes are significantly less soluble than the platinum(II) starting materials, and precipitation of product from solution results in their isolation in high purity.

An equilibrium between the platinum(II) starting materials and platinum(IV) products exists for reactions involving germanium and tin reagents. For Me$_3$SnCl, the equilibrium is shifted toward the starting materials, and hence large excesses of the tin reagent are required for the platinum(IV) species to be favored in solution. Similarly, for Me$_3$GeCl, Me$_2$SnCl$_2$, and Me$_3$SnBr there are significant amounts of both platinum(II) and platinum(IV) species present in solution, and so excess of the group 14 reagent is required to drive the reactions to completion. For other oxidative additions, the platinum(IV) product is favored and large excesses of the group 14 reagent are not required. Detailed studies of these equilibria will be presented in a future publication.

In several oxidative addition reactions of tin reagents to [PtMe$_2$(bpy-^{t}bu$_2$)], the stoichiometry is not 1:1 (Scheme 5). In the presence of excess Me$_3$SnX (X = Cl, Br), the platinum(IV) products [PtMe$_2$(Me$_3$Sn)X(bpy-^{t}bu$_2$)]·Me$_3$SnX (X = Cl, Br, I), **16**−**18**, are formed for reactions carried out in toluene. The complex [PtClMe$_2$(Me$_3$Sn)(bpy-^{t}bu$_2$)], **7b**, could be isolated by the use of only 1 equiv of Me$_3$SnCl. Compounds **A** and **B**, obtained by the oxidative additions of Me$_3$SnI and Me$_2$SnBr$_2$, respectively, to [PtMe$_2$(bpy-^{t}bu$_2$)], have a Pt:Sn ratio of 2:3, as determined by integration of ^{1}H NMR spectra and by elemental analysis. **A** was isolated as single crystals which were grown in the presence of excess Me$_3$SnI in a pentane/CH$_2$Cl$_2$ solvent system and was positively identified by X-ray structure determination as a 1:1 mixture of [PtMe$_2$(Me$_3$Sn)I(bpy-^{t}bu$_2$)] and [PtMe$_2$(Me$_3$Sn)I(bpy-^{t}bu$_2$)]·Me$_3$SnI, and **B** is formulated similarly. It thus appears that, at least for the oxidative addition of Me$_3$SnI to [PtMe$_2$(bpy-^{t}bu$_2$)], the degree of incorporation of free tin reagent in the final product is solvent dependent, with **18** being the product of toluene and **A** being the product of CH$_2$Cl$_2$.

Scheme 6

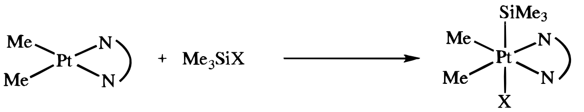

19a-d
20a-d

19a, N-N = bpy, X = Br; **19b**, N-N = bpy-^{t}bu$_2$, X = Br;
19c, N-N = py-*n*-pr, X = Br; **19d**, N-N = paen-me$_2$, X = Br;
20a, N-N = bpy, X = I; **20b**, N-N = bpy-^{t}bu$_2$, X = I;
20c, N-N = py-*n*-pr, X = I; **20d**, N-N = paen-me$_2$, X = I

Attempts to add the Si−Cl bond of Me_nSiCl_{4-n} (n = 1−3) to the platinum(II) complexes were unsuccessful, in agreement with the previous attempts by Kuyper.[10] We considered the oxidative addition of Me_3SiX (X = Br, I) to be feasible on the basis of the substantial weakening of the Si−X bond for heavier halogens.[11,12] Since platinum is a softer metal than silicon, differences in Pt−X bond strengths are expected to be less pronounced, thereby providing a thermodynamic driving force for oxidative addition of Me_3SiX (X = Br, I). Indeed, the oxidative addition of Me_3SiBr to [PtMe$_2$(diimine)] was successful, although reactions are quite slow and incomplete in some cases. The oxidative addition of Me_3SiI with all of the platinum(II) complexes **1**−**4** occurs rapidly and cleanly in both CH_2Cl_2 and toluene. Scheme 6 outlines the synthesis of the silylplatinum(IV) complexes synthesized. The absence of Si−Cl addition, the difficulty of Si−Br addition, and the ease of Si−I oxidative addition are fully consistent with the predicted halogen effect described above.[11]

Characterization of Complexes by NMR Spectroscopy.[13] The [PtMe$_2$(diimine)] complexes (**1**−**4**) give resonances in the ^{1}H NMR spectram due to the Pt−Me groups with ^2J(PtH) = 84.1−87.8 Hz, which are typical values for methylplatinum(II) complexes.[14] The ^{1}H NMR spectra of the platinum(IV) complexes [PtMe$_2$(Me$_3$E)X(diimine)] (E = Si, Ge; X = Br, I), [PtClMe$_2$(Me$_2$SnCl) (bpy-^{t}bu$_2$)], [PtBrMe$_2$(Me$_2$SnBr)(bpy-^{t}bu$_2$)]·0.5Me$_2$SnBr$_2$, and [PtClMe$_2$(MeSnCl$_2$)(paen-me$_2$)] show sharp resonances at room temperature; the spectrum of [PtIMe$_2$(Me$_3$Si)(bpy)] (**20a**) is shown in Figure 1. The ^{1}H NMR spectrum of [PtClMe$_2$(Me$_3$Ge)(bpy-^{t}bu$_2$)] shows significant line broadening, and signals due to [PtMe$_2$(bpy-^{t}bu$_2$)] and Me$_3$GeCl as well as the platinum(IV) complex are observed, indicating a reversible oxidative addition of the germanium reagent to the platinum(II) center.

The oxidative addition of Me$_3$SnCl to the dimethylplatinum(II) complexes results in an equilibrium which is shifted toward the starting materials in dilute solutions. This is readily evidenced by the purple, red, or orange colors of these complexes in solution, which arises from the Pt(5d) to π^*(diimine) MLCT band [PtMe$_2$(diimine)].[15] Room-temperature spectra show averaged chemical shifts and coupling constants for all signals. In contrast, low-temperature spectra show distinct signals for the platinum(IV) complexes and, when present (**16**, **A**), Me$_3$SnCl (δ 0.31 ppm and ^2J(SnH)$_{av}$ = 66.1 Hz).[16] Averaged signals indicate a reversible oxidative addition process which is fast on the ^{1}H NMR time scale. The ^{1}H NMR spectra of Me$_3$SnBr and Me$_3$SnI oxidative addition produces indicate similar equilibria. In the former case, significant populations of both platinum(II) and platinum(IV) species are present in solution at room temperature, although the platinum(IV) complexes are favored. In the latter case, the equilibrium is strongly shifted toward the platinum(IV) species, although exchange broadening is still evident in some cases. Exchange broadening is also seen in the spectrum of [PtClMe$_2$(Me$_2$SnCl)(paen-me$_2$)] (**9**). In all cases where exchange is seen, the spectrum of the platinum(IV) complex can be obtained at low temperature.

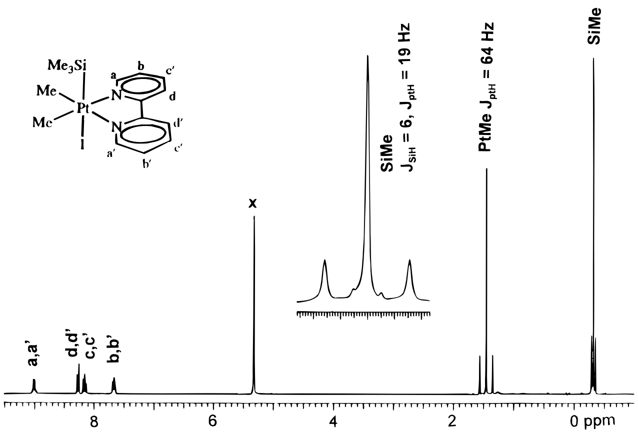

Figure 1. ^{1}H NMR spectrum of **20a** in CD_2Cl_2.

For the oxidative addition products of **4**, there are no silicon, tin, or platinum satellites associated with the NMe$_2$ signals nor are there any significant differences in the E−Me signals compared to those in the corresponding oxidative addition products of **3**. These results indicate that the NMe$_2$ group of the paen-me$_2$ ligand does not coordinate to either the group 14 element or to platinum.

Table 1 gives the Pt−Me and E−Me (E = Si, Ge, Sn) ^{1}H NMR spectral data for platinum(IV) complexes, and complete NMR data are given as Supporting Information. The platinum(IV) complexes resulting from oxidative additions to **1** and **2** have a molecular mirror plane if the addition process is *trans*. Since our platinum(IV) complexes give only one Pt−Me resonance, and the bipyridine signals indicate magnetically equivalent pyridine-like rings, one can conclude that oxidative addition has occurred in a *trans* manner. This is in accord with the known *trans* addition of the E−X (E = C, Si, Ge, Sn) bonds to **1**.[9,10,17] The unsymmetrical platinum(IV) complexes resulting from oxidative addition reactions to complexes **3** and **4** necessarily show two distinct Pt−Me signals in their ^{1}H NMR spectra, but the NMR parameters also indicate *trans* oxidative addition of E−X (E = Si, X = Br, I; E = Sn, X = Cl, Br, I).

The ^{1}H NMR spectra of all the platinum(IV) complexes show a substantial decrease in the magnitude of

---

[12] Walsh, R. *The Chemistry of Organic Silicon Compounds*; Patai, S., Rappoport, Z., Eds.; John Wiley & Sons Ltd.: Toronto, 1989; p 385.

[13] Assignments for ^{1}H NMR spectra will follow the lettering system shown in Chart 1, unless otherwise stated.

[14] (a) Monaghan, P. K.; Puddephatt, R. J. *J. Chem. Soc., Dalton Trans.* **1988**, 595. (b) Hill, R. H.; Puddephatt, R. J. *J. Am. Chem. Soc.* **1985**, *107*, 1218. (c) Monaghan, P. K.; Puddephatt, R. J. *Organometallics* **1986**, *5*, 439. (d) Crespo, M.; Puddephatt, R. J. *Organometallics* **1987**, *6*, 2548.

[15] Hill, R. H.; Puddephatt, R. J. *J. Am. Chem. Soc.* **1985**, *107*, 1218.

[16] The difference between these parameters and those of pure Me$_3$SnCl in CD$_2$Cl$_2$ (δ 0.65 ppm and ^2J(SnH)$_{av}$ = 57.3 Hz) is the result of adduct formation at low temperatures.

[17] (a) Jawad, J. K.; Puddephatt, R. J. *J. Organomet. Chem.* **1976**, *117*, 297. (b) Jawad, J. K.; Puddephatt, R. J. *J. Chem. Soc., Dalton Trans.* **1977**, 1466.

Table 1. Selected ^{1}H NMR Parameters for Platinum(IV) Complexes[a]

cpx	δ(Pt–Me) ($^2J_{PtH}$)	δ(E–Me) ($^2J_{EH}$, $^3J_{PtH}$)[b]
7a	1.10 (54.4)	−0.48 (49.2, nr)
7b	1.05 (56)	−0.37 (49.1, nr)
7c	1.18 (59.2), 1.18 (56.2)	−0.23 (45.3, nr)
7d	0.99 (58.8), 1.03 (46.7)	−0.25 (49.0, nr)
8a	1.26 (60.2)	−0.36 (51.0, nr)
8b	1.19 (59.7), 1.21 (59.9)	−0.22 (nr, nr)
8c	1.14 (60.8), 1.19 (57.8)	−0.20 (nr, nr)
9a	1.49 (61.9)	−0.25 (48.3, nr)
9b	1.40 (63.2), 1.44 (60.4)	−0.14 (48.5, nr)
9c	1.36 (63.8), 1.42 (6.13)	−0.10 (nr, nr)
10a	1.03 (54.8), 1.06 (57.4)	0.30 (50.0, 4.62)
10b	1.28 (56.5)	0.36 (48.9, nr)
11	1.34 (56.2), 1.35 (56.2)	1.08 (52.2, 5.67)
13	1.10 (62.6)	−0.27 (np, 17.6)
14	1.28 (63.1)	−0.23 (np, 17.8)
15	1.44 (64.3)	−0.28 (np, 17.8)
17	1.18 (57.9)	−0.38 (50.0, nr)
18	1.35 (59.6)	−0.44 (49.0, 10.2)
19a	1.31 (63.8)	−0.27 (6.3, 18.9)
19b	1.27 (63.7)	−0.28 (6.1, 18.9)
19c	1.24 (65.1), 1.26 (62.9)	−0.12 (6.0, 18.9)
19d	1.17 (64.6), 1.24 (63.0)	−0.13 (5.9, 18.9)
20a	1.46 (64.3)	−0.32 (6.2, 19.0)
20b	1.42 (64.1)	−0.34 (6.4, 19.1)
20c	1.37 (65.9), 1.42 (63.4)	−0.15 (6.3, 19.0)
20d	1.31 (65.2), 1.38 (63.5)	−0.17 (6.3, 19.1)
B	1.39 (57.3)	0.45 (48.3, 4.8)

[a] Solvent CD_2Cl_2; chemical shifts are given in ppm. [b] For E = Si, $^2J_{EH} = {}^2J_{^{29}Si^1H}$. *J* values in Hz. For the germanium complexes, **13**–**15**, $^2J_{EH}$ is not available. For E = Sn an average of $^2J(^{117}Sn^1H)$ and $^2J(^{119}Sn^1H)$ is given. nr = not resolved. np = not present.

the ^2J(PtH) for the Pt–Me signals when compared to the platinum(II) starting materials, as expected on going from a four-coordinate platinum(II) complex to a six-coordinate platinum(IV) complex (Table 1). For complexes of the type [$PtXMe_2(Me_3E)Pt(bpy\text{-}^tbu_2)$], ^2J(PtH) varies in the range 56–64.3 Hz, significantly smaller than for analogous alkyl complexes [$PtXMe_2R(bpy)$] (R = alkyl, X = halide), which have ^2J(PtH) typically in the range 69–72 Hz.[18,19] A decrease is also seen for the ^1J(PtC) values obtained from ^{13}C NMR spectra of these complexes. For example, ^1J(PtC) decreases from 824 Hz in [$PtMe_2(bpy\text{-}^tbu_2)$] to 612 Hz in [$PtClMe_2(Me_3Sn)Pt(bpy\text{-}^tbu_2)$].

In all but one case, the ^3J(EH) (E = Si, Sn) satellite signals flanking the Pt–Me signal in the ^{1}H NMR spectra of platinum(IV) complexes are not observed. A small coupling of ^3J(SnPtC**H**) = 5.3 Hz is seen for **11**. The presence of these satellite signals is conclusive evidence for Pt–Sn bonding in this complex. Rehybridization at the group 14 center is indicated by reduction in the magnitude of the coupling constant ^2J(ECH) (E = ^{29}Si, ^{117,119}Sn) compared to the free group-14 compounds.[20,21]

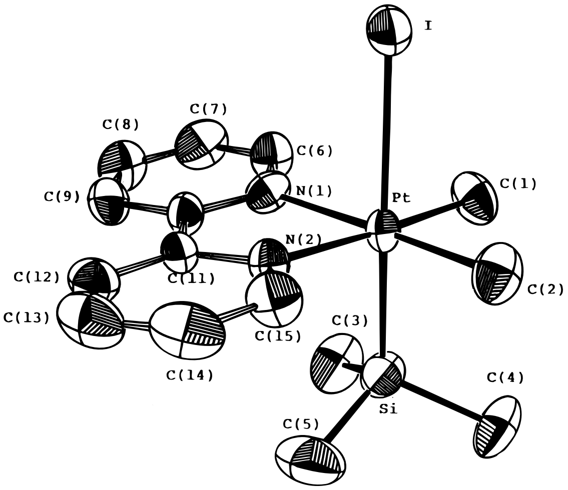

Figure 2. ORTEP view of [$PtIMe_2(Me_3Si)(bpy)$] (**20a**). Thermal ellipsoids show 50% probability levels. Hydrogen atoms are omitted for clarity.

Table 2. Selected Bond Lengths (Å) and Angles (deg) for 20a

Bond Lengths			
Pt–I	2.963(1)	Pt–Si	2.337(3)
Pt–C(1)	2.067(11)	Pt–C(2)	2.062(12)
Pt–N(1)	2.133(9)	Pt–N(2)	2.137(8)
Si–C(3)	1.885(14)	Si–C(4)	1.887(13)
Si–C(5)	1.847(17)		
Bond Angles			
I–Pt–Si	177.4(1)	I–Pt–C(1)	91.5(3)
I–Pt–C(2)	91.7(4)	I–Pt–N(1)	87.7(3)
I–Pt–N(2)	88.4(2)	Si–Pt–C(1)	86.0(4)
Si–Pt–C(2)	88.3(4)	Si–Pt–N(1)	92.6(3)
Si–Pt–N(2)	94.1(3)	C(1)–Pt–C(2)	88.7(5)
C(1)–Pt–N(1)	97.1(4)	C(1)–Pt–N(2)	174.4(4)
C(2)–Pt–N(1)	174.2(5)	C(2)–Pt–N(2)	96.9(5)
N(1)–Pt–N(2)	77.3(3)	Pt–Si–C(3)	110.5(5)
Pt–Si–C(4)	114.5(5)	Pt–Si–C(5)	110.5(5)
C(3)–Si–C(4)	107.3(6)	C(3)–Si–C(5)	106.6(7)
C(4)–Si–C(5)	107.1(7)		

Strong spectroscopic evidence for the presence of platinum–group 14 bonding in the platinum(IV) complexes is provided by the Pt–E–C–H satellite signals, ^3J(PH), associated with the E–Me ^{1}H NMR signals. For tin-containing complexes, the ^3J(PtH) satellites are not usually resolved in room-temperature spectra due to exchange broadening of the Sn–Me signal. For trimethyltin–platinum complexes, ^3J(PtH) satellite signals were only well-resolved in the low-temperature spectrum of **18** (^3J(PtH) = 10.2 Hz), but ^3J(PtH) values of 4.6, 5.7, and 4.8 Hz are readily observed in the spectra of **10a**, **11**, and **B**, respectively, i.e. complexes which contain a methylhalotin ligand. The ^3J(PtH) satellites are observed in the ^{1}H NMR spectra of silylplatinum(IV) complexes, the magnitude of which is 19.0 ± 0.1 Hz in all cases. Figure 1 shows the ^{1}H NMR spectrum of [$PtIMe_2(Me_3Si)(bpy)$] (**20a**).

Structure of [$PtIMe_2(Me_3Si)(bpy)$] (20a). An ORTEP diagram of **20a** is shown in Figure 2, and selected bond lengths and angles are in Table 2. The bpy ligand shows no exceptional features, with the two pyridine-like rings being slightly tilted [4.1(4)°] with respect to each other and with respect to the C(1), C(2), Pt, N(1), and N(2) plane [7.4(4) and 8.4(3)°]. The geometry at the platinum center is close to octahedral. The C(1)–Pt–C(2) and N(1)–Pt–N(2) angles of 88.7(5) and 77.3(3)°, respectively, are closed in from the ideal 90° octahedral angle. The atoms C(1), C(2), Pt, N(1) and N(2) form a well-defined plane. These results are consistent with the structures of similar complexes.[22]

The Pt–Si bond length in **20a** is 2.337(3) Å and is the first Pt(IV)–Si distance to be determined. The Pt–

---

(18) Crespo, M.; Puddephatt, R. J. *Organometallics* **1987**, *6*, 2548.

(19) Ferguson, G.; Monaghan, P. K.; Parvez, M.; Puddephatt, R. J. *Organometallics* **1985**, *4*, 1669.

(20) Höfler, H. *Top. Curr. Chem.* **1974**, *50*, 129.

(21) Summerville, R. H.; Hoffmann, R. *J. Am. Chem. Soc.* **1979**, *101*, 3821.

(22) For example see: Achar, S.; Scott, J. D.; Vittal, J. J.; Puddephatt, R. J. *Organometallics* **1993**, *12*, 4592.

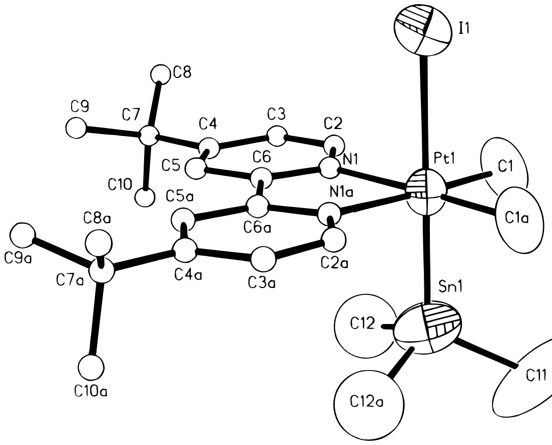

Figure 3. Structural diagram of $[PtIMe_2(Me_3Sn)(bpy\text{-}^t bu_2)]$. Thermal ellipsoids show 50% probability levels. Atoms in the bpy-^{t}bu$_2$ ligand were assigned arbitrary radii, and the hydrogen atoms were omitted.

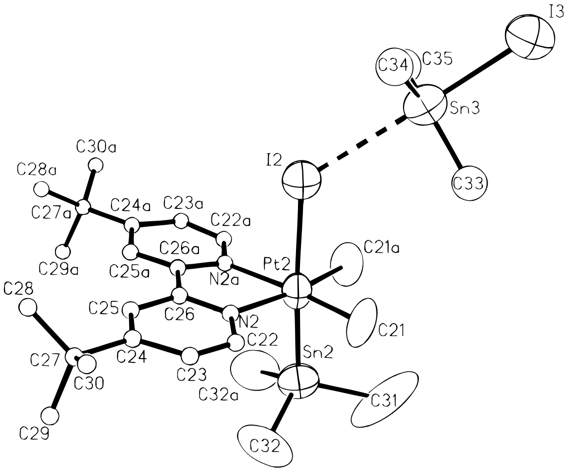

Figure 4. Structural diagram of $[PtIMe_2(Me_3Sn)(bpy\text{-}^t bu_2)]\cdot MeSnI$. Thermal ellipsoids show 50% probability levels. Atoms in the bpy-^{t}bu$_2$ ligand were assigned arbitrary radii, and the hydrogen atoms were omitted.

Table 3. Selected Bond Lengths (Å) for A

Molecule 1, $[PtIMe_2(Me_3Sn)(bpy{-}^t bu_2)]$			
Pt(1)−I(1)	2.881(4)	Pt(1)−Sn(1)	2.547(5)
Pt(1)−C(1)	2.063(26)	Pt(1)−N(1)	2.140(18)
Sn(1)−C(11)	2.200(47)	Sn(1)−C(12)	2.176(36)
Molecule 2, $[PtIMe_2(Me_3Sn)(bpy\text{-}^t bu_2)]\cdot Me_3SnI$			
Pt(2)−I(2)	2.959(4)	Pt(2)−Sn(2)	2.567(4)
Pt(2)−C(21)	2.048(24)	Pt(2)−N(2)	2.115(21)
Sn(2)−C(31)	2.289(50)	Sn(2)−C(32)	2.128(31)
I(3)−Sn(3)	2.809(5)	I(2)−Sn(3)	3.385(4)
Sn(3)−C(33)	2.106(43)	Sn(3)−C(34)	2.106(44)
Sn(3)−C(35)	2.106(28)	Sn(3)−C(36)	2.106(75)
Sn(3)−C(37)	2.106(49)		

Table 4. Selected Bond Angles (deg) for A

Molecule 1, $[PtIMe_2(Me_3Sn)(bpy\text{-}^t bu_2)]$			
I(1)−Pt(1)−Sn(1)	179.6(1)	I(1)−Pt(1)−C(1)	92.2(7)
Sn(1)−Pt(1)−C(1)	88.1(8)	I(1)−Pt(1)−N(1)	87.6(5)
Sn(1)−Pt(1)−N(1)	92.2(5)	C(1)−Pt(1)−N(1)	97.5(9)
I(1)−Pt(1)−C(1A)	92.2(7)	Sn(1)−Pt(1)−C(1A)	88.1(8)
C(1)−Pt(1)−C(1A)	88.1(14)	N(1)−Pt(1)−C(1A)	174.5(9)
I(1)−Pt(1)−N(1A)	87.6(5)	Sn(1)−Pt(1)−N(1A)	92.2(5)
C(1)−Pt(1)−N(1A)	174.5(9)	N(1)−Pt(1)−N(1A)	77.0(10)
C(1A)−Pt(1)−N(1A)	97.5(9)	Pt(1)−Sn(1)−C(11)	116.8(17)
Pt(1)−Sn(1)−C(12)	108.0(10)	C(11)−Sn(1)−C(12)	107.8(13)
Pt(1)−Sn(1)−C(12A)	108.0(10)	C(11)−Sn(1)−C(12A)	107.8(13)
C(12)−Sn(1)−C(12A)	108.1(18)		
Molecule 2, $[PtIMe_2(Me_3Sn)(bpy\text{-}^t bu_2)]\cdot Me_3SnI$			
I(2)−Pt(2)−Sn(2)	176.9(1)	I(2)−Pt(2)−C(21)	91.7(8)
Sn(2)−Pt(2)−C(21)	86.2(8)	I(2)−Pt(2)−N(2)	87.1(5)
Sn(2)−Pt(2)−N(2)	95.4(5)	C(21)−Pt(2)−N(2)	95.8(9)
I(2)−Pt(2)−C(21A)	91.7(8)	Sn(2)−Pt(2)−C(21A)	86.2(8)
C(21)−Pt(2)−C(21A)	93.6(14)	N(2)−Pt(2)−C(21A)	170.5(9)
I(2)−Pt(2)−N(2A)	87.1(5)	Sn(2)−Pt(2)−N(2A)	95.4(5)
C(21)−Pt(2)−N(2A)	170.5(9)	N(2)−Pt(2)−N(2A)	74.7(11)
C(21A)−Pt(2)−N(2A)	95.8(9)	Pt(2)−I(2)−Sn(3)	124.5(1)
Pt(2)−Sn(2)−C(31)	107.8(15)	Pt(2)−Sn(2)−C(32)	108.8(8)
C(31)−Sn(2)−C(32)	109.8(11)	Pt(2)−Sn(2)−C(32A)	108.8(8)
C(31)−Sn(2)−C(32A)	109.8(11)	C(32)−Sn(2)−C(32A)	111.9(17)
Pt(2)−N(2)−C(22)	125.5(17)	Pt(2)−N(2)−C(26)	116.9(16)
I(2)−Sn(3)−I(3)	178.9(1)	I(2)−Sn(3)−C(33)	87.5(15)
I(2)−Sn(3)−C(34)	89.3(15)	I(2)−Sn(3)−C(35)	88.3(15)
I(2)−Sn(3)−C(36)	79.6(24)	I(2)−Sn(3)−C(37)	79.8(17)
I(3)−Sn(3)−C(33)	93.5(14)	I(3)−Sn(3)−C(34)	89.8(14)
I(3)−Sn(3)−C(35)	91.6(15)	I(3)−Sn(3)−C(36)	99.3(24)
I(3)−Sn(3)−C(37)	100.8(18)	C(33)−Sn(3)−C(34)	119.9(16)
C(33)−Sn(3)−C(35)	119.9(17)	C(34)−Sn(3)−C(35)	119.9(18)
C(36)−Sn(3)−C(37)	120.0(16)	C(37)−Sn(3)−C(37A)	110.6(32)

Si bond length is similar to those seen for R_3Si ligands *trans* to halides in platinum(II) complexes; the Pt−Si bond lengths are 2.317(2) Å for (+)-*trans*-$[PtCl\{SiMe(1\text{-}C_{10}H_7)Ph\}(PMe_2Ph)_2]$[23] and 2.330(17) Å for *trans*-$[PtBr(Me_3Si)OPEt_3)_2]$.[24]

The most remarkable feature seen in the structure of **20a** is the exceptionally long Pt−I bond length of 2.963(1) Å. This is by far the longest single Pt−I bond length ever reported; the structure of $[PtIMe_3\{(PPh_2)CH(PPh_2)CH_2NHCH_2Ph\}]$,[25] where the iodo ligand is *trans* to a methyl group, has the next longest bond known to date (2.853(6) Å). On the basis of published structures,[25−30] the high *trans*-influence of the methyl group causes Pt−I bond lengthenings of 0.13−0.21 Å compared to the sum of the covalent radii of 2.64 Å for platinum and iodine.[31] The Pt−I bond length in **20a** is 0.32 Å longer than the sum of the covalent radii of the two atoms. The substantially longer Pt−I bond length in **20a** compared to those seen for complexes where the iodo ligand is *trans* to a methyl group indicates a substantially larger *trans*-influence of the trimethylsilyl group compared to the methyl group.[32]

Structure of $[PtIMe_2(Me_3Sn)(bpy\text{-}^t bu_2)]_2\cdot Me_3SnI\cdot CH_2Cl_2$ (A). The structure of **A** is shown in Figures 3 and 4, and selected bond parameters and bond angles are listed in Tables 3, and 4, respectively. Two distinct complexes are present (1:1 ratio) in the unit cell. The first is the simple *trans* oxidative addition product of Me_3SnI to $[PtMe_2(bpy\text{-}^t bu_2)]$ (Figure 3), and the second is $[PtIMe_2(Me_3Sn)(bpy\text{-}^t bu_2)]\cdot Me_3SnI$ (Figure 4). In this second complex the platinum-bound iodo ligand coordinates to the tin center of the Me_3SnI molecule to give a trigonal-bpyramidal tin center. A highly disordered molecule of CH_2Cl_2 is also presented in the unit cell.

---

(23) Hitchcock, P. B. *Acta Crystallogr.* **1976**, *B32*, 2014.

(24) Yamashita, H.; Hayashi, T.; Kobayashi, T.; Tanaka, M.; Goto, M. *J. Am. Chem. Soc.* **1988**, *110*, 4417.

(25) Hassan, F. S. M.; Higgins, S. J.; Jacobsen, G. B.; Shaw, B. L.; Thornton-Pett, M. *J. Chem. Soc., Dalton Trans.* **1988**, 3011.

(26) Clark, H. C.; Ferguson, G.; Jain, V. K.; Parvez, M. *J. Organomet. Chem.* **1984**, *270*, 365.

(27) Abel, E. W.; Bhargava, S. K.; Orrell, K. G.; Platt, A. W. G.; Sik, V.; Cameron, T. S. *J. Chem. Soc., Dalton Trans.* **1985**, 345.

(28) Abel, E. W.; Coston, T. P. J.; Higgins, K. M.; Orrell, K. G.; Sik, V.; Cameron, T. S. *J. Chem. Soc., Dalton Trans.* **1989**, 701.

(29) Abel, E. W.; Moss, I.; Orrell, K. G.; Sik, V.; Stephenson, D.; Bates, P. A.; Hursthouse, M. B. *J. Chem. Soc., Dalton Trans.* **1988**, 521.

(30) Casalone, G.; Mason, R. *Inorg. Chim. Acta* **1973**, *7*, 429.

(31) Pauling, L. *The Nature of the Chemical Bond*, 3rd ed.; Cornell Univ. Press: Ithaca, NY, 1960.

(32) Chatt, J.; Eaborn, C.; Ibekwe, S. *J. Chem. Soc., Chem. Commun.* **1966**, 700.

The atoms Pt(1), C(1), C(2), and N(1,1a) of [$PtIMe_2(Me_3Sn)(bpy\text{-}^tbu_2)$] (Figure 3) form a plane, and there are no unusual features in the bonding of the bpy-^{t}bu$_2$ or methyl ligands to platinum. The Pt−Sn bond length is 2.547(5) Å, and this is the first crystallographic determination of a trimethyltin−platinum bond length. The structure of only one other platinum(IV)−tin complex has been determined.[33] In that case, the Pt−Sn bond distance for a (p-$MeC_6H_4)_3Sn$ group *trans* to a (p-$MeC_6H_4)_2Sn$ group was found to be 2.645(1) Å, considerably longer than that found for [$PtIMe_2(Me_3Sn)(bpy\text{-}^tbu_2)$]. Several structures of complexes with platinum(II)−tin bonds have been determined, and the Pt−Sn bond lengths in these complexes range from 2.48 to 2.63 Å.[34−36]

Trimethyltin unit in [$PtIMe_2(Me_3Sn)(bpy\text{-}^tbu_2)$] is bent slightly toward the Me−Pt−Me moiety as was seen for the trimethylsilyl group of [$PtIMe_2(Me_3Si)(bpy)$]. The Pt−I bond length in [$PtIMe_2(Me_3Sn)(bpy\text{-}^tbu_2)$] is found to be 2.881(4) Å. This is more than 0.08 Å shorter than was found for the analogous [$PtIMe_2(Me_3Si)(bpy)$] complex, indicating the weaker *trans*-influence of the trimethyltin compared to the trimethylsilyl ligand. When compared to the Pt−I bond lengths for iodo group *trans* to methyl ligands, our result indicates that the *trans*-influence follows the sequence $Me_3Si > Me_3Sn > Me$.

A view of the [$PtIMe_2(Me_3Sn)bpy\text{-}^tbu_2)$]·$Me_3SnI$ unit of **A** is shown in Figure 4. As for [$PtIMe_2(Me_3Sn)(bpy\text{-}^tbu_2)$], the methyl groups of the trimethyltin and bpy-^{t}bu$_2$ groups are disordered with respect to the molecular plane; the methyl groups of the Me_3SnI unit show 3-fold disorder. The most interesting feature of the second complex is the iodo ligand coordination to the Me_3SnI unit to give a trigonal-bipyramidal tin center. Bridging halide interactions such as the one described here are not uncommon in organotin chemistry, and triorganotin halides have a marked tendency to increase their coordination numbers to 5. Me_3SnF is known to have planar trimethyltin groups with nonlinear asymmetric Sn−F- - -Sn bridges.[37] A similar structure is seen for Me_3SnCl in the solid state.[38] Triorganotin bromides and iodides are weaker Lewis acids than their fluoro and chloro analogs, and this property, coupled with their large size, favors a monomeric tetrahedral structure in the solid state, as found crystallographically for Ph_3SnBr.[39] However, ^{119m}Sn Mössbauer spectroscopy indicates that, at 80 K, the lower trialkyltin bromides and iodides adopt polymeric structures containing five-coordinate tin centers.[40] Our structure appears to support the latter study and provides the first crystallographically characterized I−Sn- - -I linkage involving a triorganotin group.

The Me_3SnI unit of [$PtIMe_2(Me_3Sn)(bpy\text{-}^tbu_2)$]·$Me_3SnI$ has the three methyl groups in the equatorial plane, analogous to the structure of Me_3SnF.[37] The trimethyltin unit is close to planar, but there is a slight closing of the C−Sn(3)−I(2) angles from 90°, consistent with the weaker Sn−I interaction involving the bridging iodide. The I−Sn−I bond angle in the complex is very close to linear [(178.9(1)°]. The Sn−I bond lengths are unsymmetrical for the terminal iodine [2.809(5) Å] and for the bridging iodine [3.385(4) Å]. The Pt(2)−I(2)−Sn(3) angle is 124.5(1)°.

Conclusions

We have successfully synthesized and characterized a wide range of novel platinum(IV) complexes by the oxidative addition of E−X (E = Ge, Sn; X = Cl, Br, I; E = Si; X = Br, I) to platinum(II) complexes of the type [$PtMe_2$(diimine)]. These reactions, with the exception of some involving Me_3SiBr, are exceptionally rapid when compared to other oxidative additions to platinum(II). The complexes [$PtXMe_2(Me_3Si)$(diimine)] (X = Br, I) represent the first examples of silicon−halide oxidative addition to platinum(II), as well as the first well-characterized silylplatinum(IV) complex.

A number of the novel complexes and compounds crystallize as adducts between a platinum(IV) complex and an organohalotin compound. This is a new bonding arrangement in which the platinum-bound iodo ligand coordinates to the tin center of the organohalotin compound to give a five-coordinate, trigonal-bipyramidal tin center. This is the first time a tin center has been conclusively shown to have adopted such a geometry as the result of iodide coordination.

The determination of the X-ray crystal structures of **20a** and **A** provide an indication of the degree of the *trans*-influence exerted by the trimethyltin and trimethylsilyl ligands, the sequence being $Me_3SiI > Me_3Sn > Me$. Our results indicate that trimethyltin has a somewhat higher *trans*-influence than a methyl group. The trimethylsilyl group shows an exceptionally high *trans*-influence, as evidenced by the extremely long Pt−I bond length of 2.963(1) Å of the *trans* iodo ligand. The Pt−I distance [2.959(4) Å] is significantly longer than in [$PtIMe_2(Me_3Sn)(bpy\text{-}^tbu_2)$], no doubt due to the coordination of the iodide to tin.

Experimental Section

General Information. ^{1}H NMR spectra were recorded using Varian XL 200, Gemini 200, or Gemini 300 spectrometers. ^{13}C spectra were obtained using a Gemini 300 spectrometer, and ^{195}Pt spectra were obtained using a Varian XL 300 spectrometer. VT NMR experiments were performed on a Varian Gemini 300 spectrometer. Chemical shifts for ^{1}H and ^{13}C spectra are reported in ppm using the residual solvent nuclei as references. Infrared spectra were recorded on a Perkin-Elmer 2000 FT-IR spectrometer. All elemental analyses were performed by Guelph Chemical Laboratories. Unless

---

(33) Almeida, J. F.; Dixon, K. R.; Eaborn, C.; Hitchcock, P. B.; Pidcock, A.; Vinaixa, J. *J. Chem. Soc., Chem. Commun*. **1982**, 1315.

(34) (a) Albinati, A.; Nägeli, R.; Rüegger, H.; Pregosin, P. S. *Angew. Chem., Int. Ed. Engl*. **1982**, *21*, 284. (b) Albinati, A.; Nägeli, R.; Ostoja, K. H. A.; Starzewski, P. S.; Pregosin, P. *Inorg. Chim. Acta* **1983**, *76*, L231. (c) Albinati, A.; Pregosin, P. S.; Rüegger, H. *Inorg. Chem*. **1984**, *23*, 3223. (d) Albinati, A.; Pregosin, P. S.; Rüegger, H. *Angew. Chem., Int. Ed. Engl*. **1984**, *23*, 78. (e) Albinati, A.; Moriyama, H.; Rüegger, H.; Pregosin, P. S.; Togni, A. *Inorg. Chem*. **1985**, *24*, 4430. (f) Albinati, A.; Von Gunten, U.; Pregosin, P. S.; Guegg, H. J. *J. Organomet. Chem*. **1985**, *295*, 239. (g) Musco, A.; Pontellini, R.; Grassi, M.; Sironi, A.; Meille, S. V.; Rüegger, H.; Ammann, C.; Pregosin, P. S. *Organometallics* **1988**, *7*, 2130. (h) Grassi, M.; Meille, S. V.; Musco, A.; Pontellini, R.; Sironi, A. *J. Chem., Soc. Dalton Trans*. **1989**, 615. (i) Grassi, M.; Meille, S. V.; Musco, A.; Pontellini, R. *J. Chem. Soc., Dalton Trans*. **1990**, 251.

(35) (a) Alcock, N. W.; Nelson, J. H. *J. Chem. Soc., Dalton Trans*. **1982**, 2415. (b) Nelson, J. H.; Alcock, N. W. *Inorg. Chem*. **1982**, *21*, 1196.

(36) Goel, A. B.; Goel, S.; Vanderveer, D. *Inorg. Chim. Acta* **1981**, *54*, L5.

(37) Clark, H. C.; O'Brien, R. J.; Trotter, J. *J. Chem. Soc*. **1964**, 2332.

(38) Hossain, M. B.; Lefferts, J. L.; Molloy, K. C.; Van der Helm, D.; Zuckerman, J. J. *Inorg. Chim. Acta* **1979**, *36*, L409.

(39) Preut, H.; Huber, F. *Acta Crystallogr*. **1979**, *B35*, 744.

(40) Murdock, A. G.; Platt, R. H. *J. Chem. Soc. A* **1971**, 1191.

otherwise specified, ^{1}H NMR spectral assignments are made according to the labeling scheme in Figure 1.

Preparation of Diimine Ligands. 2,2′-Bipyridyl (bpy) was purchased (Aldrich) and used without further purification. 4,4′-Di-*tert*-butyl-2,2′-bipyridyl (bpy-^{t}bu$_2$) was synthesized by previously reported methods.[41] (2-Imino-*n*-propyl)pyridine (py-*n*-pr)[42] and *N*-(*β*-*N*′,*N*′-dimethylaminoethyl)pyridinealdehyde (paen-me$_2$)[43] were synthesized in quantitative yields by modified literature methods. (2-Imino-*n*-propyl)pyridinecarboxaldehyde was synthesized according to the following procedure: To a stirred diethyl ether (50 mL) solution of 2-pyridinecarboxaldehyde (3.61 g, 33.7 mmol) was added propylamine (1.99 g, 33.7 mmol). Anhydrous $MgSO_4$ (5 g) was added, and the suspension was stirred for 1 h. The solid was removed by filtration, and the solvent was removed from the resulting solution under vacuum. Pumping at 0.03 Torr for 20 h was required to remove the last traces of ether from the yellow oil. The yield of product was quantitative. The density of the liquid was determined to be 0.986 g/mL at 20 °C. ^{1}H NMR (C_6D_6): δ 0.89 [t, 3H, $^3J(H^gH^h) = 7.40$ Hz, H^h], δ 1.66 [q (br), 2H, H^g], δ 3.46 [td, 2H, $^3J(H^fH^g) = 6.78$ Hz, $^4J(H^eH^f) = 1.46$ Hz, H^f], δ 6.74 [ddd, 1H, $^3J(H^bH^c) = 7.25$ Hz, $^3J(H^aH^b) = 4.76$ Hz, $^4J(H^bH^d) = 1.10$ Hz, H^b], δ 7.16 [m, 1H, H^c], δ 8.17 [m, 1H, $^3J(H^cH^d) = 7.88$ Hz, H^d], δ 8.52 [m, 1H, H^a], δ 8.54 [s, 1H, H^e]. *N*-(*β*-*N*′,*N*′-dimethylaminoethyl)pyridinecarboxaldehyde was synthesized according to the same procedure except that 2-pyridinecarboxaldehyde (2.25 g, 21.0 mmol) and *N*,*N*-dimethylethylenediamine (1.85 g, 21.0 mmol) were used. The density of the liquid was found to be 0.988 g/mol at 20 °C. ^{1}H NMR (C_6D_6): δ 2.08 [s, 6H, H^h], δ 2.53 [t, 2H, $^3J(H^fH^g) = 6.77$ Hz, H^g], δ 3.62 [td, 2H, $^4J(H^eH^f) = 1.43$ Hz, H^f], δ 6.66 (ddd, 1H, $^3J(H^bH^c) = 7.46$ Hz, $^3J(H^aH^b) = 4.85$ Hz, $^4J(H^bH^d) = 1.28$ Hz, H^b], δ 7.07 [dddd, 1H, $^3J(H^cH^d) = 7.95$ Hz, $^4J(H^aH^c) = 1.77$ Hz, $^5J(H^cH^e) = 0.72$ Hz, H^c], δ 8.13 [dt, 1H, $^3J(H^cH^d) = 6.81$ Hz, H^d], δ 8.47 [ddd, 1H, $^5J(H^aH^d) = 0.98$ Hz, H^a], δ 8.53 [td, 1H, $^4J(H^dH^c) = 0.73$ Hz, H^e].

Preparation of Dimethylplatinum(II) Complexes. All dimethylplatinum(II) complexes were prepared by adding the appropriate diimine ligand to a solution of $[Pt_2Me_4(\mu\text{-}SMe_2)_2]$.[44,45] [PtMe$_2$(bpy)] (**1**)[46] and [PtMe$_2$(bpy-^{t}bu$_2$)] (**2**)[41] were synthesized according to the established procedures. [PtMe$_2$(py-*n*-pr)] (**3**) was prepared according to the following procedure: To a stirred suspension of $[Pt_2Me_4(\mu\text{-}SMe_2)_2]$ (0.500 g, 0.87 mmol) in diethyl ether (10 mL) was added 2.2 equiv of (2-imino-*n*-propyl)pyridine (0.258 g, 1.74 mmol). An immediate reaction occurred, and a deep red-purple microcrystalline solid precipitated from solution. The reaction mixture was stirred for 1 h, after which time it was filtered. The solid was washed with hexane to remove traces of excess ligand and then dried *in vacuo*. Yield: 92%. Anal. Calcd for $C_{11}H_{18}N_2Pt$: C, 35.03; H, 4.67; N, 7.31. Found: C, 35.39; H, 4.86; N, 7.50. ^{1}H NMR in CD_2Cl_2: δ 0.954 [t, 3H, $^3J(H^gH^h) = 14.8$ Hz, H^h], δ 1.05 [s, 3H, ^2J(PtH) = 87.5 Hz, Pt−Me], δ 1.10 [s, 3H, ^2J(PtH) = 84.1 Hz, Pt−Me], δ 1.88 [m, 2H, H^g], δ 4.03 [t, 2H, $^3J(H^fH^g) = 7.15$ Hz, $^3J(PtH^f) = 20.3$ Hz, H^f], δ 7.59 [ddd, 1H, $^3J(H^bH^c) = 5.50$ Hz, $^3J(H^aH^b) = 7.63$ Hz, $^4J(H^bH^d) = 1.31$ Hz, H^b], δ 7.69 [dd, 1H, $^3J(H^cH^d) = 7.69$ Hz, H^d], δ 8.10 [dtd, 1H, $^3J(H^aH^c) = 1.43$, H^c], δ 9.11 [s, 1H, $^3J(PtH^e) = 35.7$ Hz, H^e], δ 9.17 [d, $^3J(PtH^a)$ = 19.4 Hz, H^a]. [PtMe$_2$(paen-me$_2$)] (**4**) was prepared by using the same procedure. Yield: 95%. Anal. Calcd for $C_{12}H_{21}N_3Pt$: C, 35.44; H, 5.08; N, 10.18. Found: C, 35.82; H, 5.26; N, 10.44. ^{1}H NMR in CD_2Cl_2: δ 1.03 [s, 3H, ^2J(PtH) = 87.8 Hz, Pt−Me], δ 1.10 [s, 3H, ^2J(PtH) = 84.3 Hz, Pt−Me], δ 2.26 [s, 6H, H^h], δ 2.72 [m, 2H, $^3J(H^fH^g) = 6.23$ Hz, H^g], δ 4.16 [m, 2H, $^3J(PtH^f) = 19.7$ Hz, H^f], δ 7.58 [m, 1H, H^b], δ 7.70 [m, 1H, H^d], δ 8.10 [m, 1H, H^c], δ 9.12 [s, 1H, $^3J(PtH^e) = 35.3$ Hz, H^e], δ 9.16 [d, 1H, $^3J(H^aH^b) = 5.4$ Hz, $^3J(PtH^a) = 19.3$ Hz, H^a].

Preparation of Mono- and Dihaloplatinum(II) Complexes. [PtClMe(bpy)],[47] [PtBrMe(bpy)],[10] [PtIMe(bpy)],[46] [PtCl$_2$(bpy)], and [PtX$_2$(bpy)] (X = Cl, Br, I)[48] were prepared by modifications of previously reported syntheses, with platinum−dimethyl sulfide complexes being used in place of the platinum−cyclooctadiene precursor complexes. [PtClMe(SMe$_2$)$_2$], [PtBrMe(SMe$_2$)$_2$], [PtIMe(SMe$_2$)$_2$], [PtBr$_2$(SMe$_2$)$_2$], and [PtI$_2$(SMe$_2$)$_2$] were prepared according to the procedures of Scott and Puddephatt.[44] ^{1}H NMR assignments for complexes of the type [PtXMe(bpy-^{t}bu$_2$)] follow the labeling system in Chart 1 with H^{a-d} representing signals due to protons on the pyridine ring *trans* to the methyl group and H$^{a-d'}$ representing signals due to protons on the pyridine ring *trans* to the halide ligand.

[PtClMe(bpy-^{t}bu$_2$)] (5a). [PtClMe(SMe$_2$)$_2$] (50.0 mg, 0.135 mmol) was dissolved in acetone [3 mL) and bpy-^{t}bu$_2$ (40.0 mg, 0.149 mmol) was then added, resulting in an immediate color change of the solution from pale to bright yellow. After 90 min, a yellow precipitate had formed and hexane (10 mL) was added. The solid was isolated by filtration, washed with hexane, and dried *in vacuo*. The yield of microcrystalline yellow solid was 79%. Anal. Calcd for $C_{19}H_{27}ClN_2Pt$: C, 44.40; H, 5.29; N, 5.45. Found: C, 44.10; H, 5.31; N, 5.27. ^{1}H NMR ($CDCl_3$): δ 1.13 [s, 3H, ^2J(PtH) = 77.9 Hz, Pt−Me], δ 1.41 [s, 9H, H$^{c'}$], δ 1.42 [s, 9H, H^c], δ 7.41 [dd, 1H, $^3J(H^{a'}H^{b'}) = 6.23$ Hz, $^4J(H^{b'}H^{d'}) = 2.20$ Hz, H$^{b'}$], δ 7.56 [dd, 1H, $^3J(H^aH^b) = 5.86$ Hz, $^4J(H^aH^d) = 1.89$ Hz, H^b], δ 7.86 [d, 1H, H$^{d'}$], δ 7.88 [d, 1H, H^d], δ 9.01 [d, 1H, $^3J(PtH^{a'}) = 59.6$ Hz, H$^{a'}$], δ 9.43 [d, 1H, $^3J(PtH^a) = 12$ Hz, H^a]. The same procedure was followed for the syntheses of [PtBrMe(bpy-^{t}bu$_2$)] (**5b**) and [PtIMe(bpy-^{t}bu$_2$)] (**5c**). **5b**: The yield of yellow solid was 58%. Anal. Calcd for $C_{19}H_{27}BrN_2Pt$: C, 40.87; H, 4.87; N, 5.02. Found: C, 41.02; H, 4.90; N, 4.93. ^{1}H NMR (acetone-*d*$_6$): δ 1.04 [s, 3H, ^2J(PtH) = 78.2 Hz, Pt−Me], δ 1.44 [s, 9H, H$^{c'}$], δ 1.45 [s, 9H, H^c], δ 7.72 [dd, 1H, $^3J(H^{a'}H^{b'}) = 6.22$ Hz, $^4J(H^{b'}H^{d'}) = 2.19$ Hz, H$^{b'}$], δ 7.79 [dd, 1H, $^3J(H^aH^b) = 5.90$ Hz, $^4J(H^aH^d) = 1.99$ Hz, H^b], δ 8.49 [d, 1H, H$^{d'}$], δ 8.52 [d, 1H, H^d], δ 9.02 [d, 1H, $^3J(PtH^{a'})$ = 59.5 Hz, Ha′], δ 9.59 [d, 1H, $^3J(PtH^a) = 13.6$ Hz, H^a]. **5c**: The yield of yellow solid was 52%. Anal. Calcd for $C_{19}H_{27}IN_2Pt$: C, 37.67; H, 4.50; N, 4.63. Found: C, 37.52; H, 4.52; N, 4.43. ^{1}H NMR (acetone-*d*$_6$): δ 1.06 [s, 3H, ^2J(PtH) = 76.5 Hz, Pt−Me], δ 1.44 [s, 9H, H$^{c'}$], δ 1.46 [s, 9H, H^c], δ 7.73 [dd, 1H, $^3J(H^{a'}H^{b'}) = 6.37$ Hz, $^4J(H^{b'}H^{d'}) = 1.79$ Hz, H$^{b'}$], δ 7.78 [dd, 1H, $^3J(H^aH^b) = 6.37$ Hz, $^4J(H^bH^d) = 2.20$ Hz, H^b], δ 8.50 [d, 1H, H$^{d'}$], δ 8.51 [d, 1H, H^d], δ 8.94 [d, 1H, $^3J(PtH^{a'}) = 56.8$ Hz, H$^{a'}$], δ 9.83 [d, 1H, $^3J(PtH^a) = 16.5$ Hz, H^a].

[PtCl$_2$(bpy-^{t}bu$_2$)] (6a). K$_2$[PtCl$_4$] (78.0 mg, 0.188 mmol) and bpy-^{t}bu$_2$ (59.0 mg, 0.222 mmol) were refluxed in a solution of water (10 mL), concentrated HCl (5 mL), and acetone (10 mL) for 20 h. The resulting yellow solid was isolated by filtration. Yield: 73%. Anal. Calcd for $C_{18}H_{24}Cl_2N_2Pt$: C, 40.46; H, 4.53; N, 5.24. Found: C, 40.71; H, 4.60; N, 5.22. ^{1}H NMR ($CDCl_3$): δ 1.44 [s, 18H, H^c], δ 7.47 [dd, 2H, $^3J(H^aH^b)$ = 6.27 Hz, $^4J(H^bH^d) = 1.06$ Hz, H^b], δ 7.87 [d, 2H, H^d], δ 9.48 [d, 2H, $^3J(PtH^a) = 39.8$ Hz, H^a].

[PtBr$_2$(bpy-^{t}bu$_2$)] (6b). [PtBr$_2$(SMe$_2$)$_2$] (167 mg, 0.349 mmol) was dissolved in acetone (10 mL), and bpy-^{t}bu$_2$ (103 mg, 0.384 mmol) was added. The solution was stirred for 2 h, after which time a yellow precipitate had formed. Hexane (10 mL) was added, and the solid was isolated by filtration, washed with hexane, and dried *in vacuo*. Yield: 82%. Anal. Calcd for $C_{18}H_{24}Br_2N_2Pt$: C, 34.69; H, 3.88; N, 4.49. Found: C, 34.59; H, 3.85; N, 4.44. ^{1}H NMR (acetone-*d*$_6$): δ 1.45 [s, 18H, H^c], δ 7.56 [dd, 2H, $^3J(H^aH^b) = 6.37$ Hz, $^4J(H^bH^d) = 2.20$ Hz, H^b], δ 7.92 [d, 2H, H^d], δ 9.80 [d, 2H, $^3J(PtH^a) = 40.3$ Hz, H^a].

---

[41] Achar, S.; Scott, J. D.; Vittal, J. J.; Puddephatt, R. J. *Organometallics* **1993**, *12*, 4592.

[42] Bamfield, P.; Price, R.; Miller, R. G. J. *J. Chem. Soc. A* **1969**, 1447.

[43] Buffin, B. P.; Richmond, T. G. *Polyhedron* **1990**, *9*, 2887.

[44] Scott, J. D.; Puddephatt, R. J. *Organometallics* **1983**, *2*, 1643.

[45] Hill, G. S.; Irwin, M. J.; Levy, C. J.; Rendina, L. M.; Puddephatt, R. J. *Inorg. Synth*., in press.

[46] Monaghan, P. K.; Puddephatt, R. J. *Organometallics* **1984**, *3*, 444.

[47] Clark, H. C.; Manzer, L. E. *J. Organomet. Chem.* **1973**, *59*, 411.

[48] Gidney, P. M.; Gillard, R. D.; Heaton, B. T. *J. Chem. Soc., Dalton Trans.* **1973**, 132.

[PtI$_2$(bpy-^{t}bu$_2$)] (**6c**) was synthesized using the same procedure. **6c**: Yield 85%. Anal. Calcd for $C_{18}H_{24}I_2N_2Pt$: C, 30.14; H, 3.37; N, 3.91. Found: C, 30.30; H, 3.33; N, 3.88. ^{1}H NMR (CDCl$_3$): δ 1.45 [s, 18H, H^d], δ 7.46 [dd, 2H, $^3J(H^aH^b) = 6.27$ Hz, $^4J(H^bH^c) = 2.16$ Hz, H^b], δ 7.89 [d, 2H, H^c], δ 10.03 [d, 1H, $^3J(PtH^a) = 39.2$ Hz, H^a].

Synthesis of Platinum(IV) Complexes. All procedures were carried out under a nitrogen atmosphere by means of a Vacuum Atmospheres Mo-40-1 drylab. CH$_2$Cl$_2$ was dried over CaH$_2$, and all other solvents were dried over sodium/benzophenone. Trimethyltin iodide was prepared by halogen exchange from trimethyltin chloride according to the literature procedure.[49] Trimethylgermanium iodide was synthesized from tetramethylgermane according to the literature procedure.[50] All other tin and silicon reagents were purchased from Aldrich and used without further purification. Germanium reagents were purchased from Gelest and used without further purification.

[PtClMe$_2$(Me$_3$Sn)(bpy)] (7a). This is a modification of the literature method.[9] To a solution of [PtMe$_2$(bpy)] (0.100 H, 0.262 mmol) in CH$_2$Cl$_2$ (2 mL) was added Me$_3$SnCl (0.105 g, 0.524 mmol). The solution became lighter in color, and the solvent was removed *in vacuo* to afford an off-white solid. The solid was suspended in toluene and isolated by filtration. The product was then washed with toluene and dried *in vacuo*. Yield: 97%. [PtBrMe$_2$(Me$_3$Sn)(bpy)] (**8a**), [PtIMe$_2$(Me$_3$Sn)(bpy)] (**9a**), [PtBrMe$_2$(Me$_3$Si)(bpy)] (**19a**), and [PtIMe$_2$(Me$_3$Si)(bpy)] (**20a**) were synthesized by the same procedure. **8a**: Yield 89%. Anal. Calcd for $C_{15}H_{23}BrN_2PtSn$: C, 28.82; H, 3.71; N, 4.48. Found: C, 29.07; H, 3.84; N, 4.56. **9a**: Yield 87%. Anal. Calcd for $C_{15}H_{23}IN_3PtSn$: C, 26.81; H, 3.34; N, 4.17. Found: C, 27.17; H, 3.39; N, 4.39. **19a**: yield 74%. Anal. Calcd for $C_{15}H_{23}BrN_2PtSi$: C, 33.71; H, 4.34; N, 5.24. Found: C, 33.51; H, 3.99; N, 5.18. **20a**: Yield 93%. Anal. Calcd for $C_{15}H_{28}IN_2PtSi$: C, 30.99; H, 3.99; N, 4.82. Found: C, 31.26; H, 3.51; N, 4.61.

[PtClMe$_2$(Me$_3$Sn)(bpy-^{t}bu$_2$)] (7b). To a stirred solution of [PtMe$_2$(bpy-^{t}bu$_2$)] (52.5 mg, 0.106 mmol) in CH$_2$Cl$_2$ (1 mL) was added Me$_3$SnCl (21.2 mg, 0.106 mmol). The solution was cooled to 0 °C, and the solvent was removed *in vacuo* to give an off-white solid. Yield: 85%. Anal. Calcd for $C_{23}H_{39}ClN_2PtSn$: C, 39.87; H, 5.67; N, 4.04. Found: C, 39.79; H, 5.67; N, 4.03. [PtClMe$_2$(Me$_3$Sn)(py-*n*-pr)] (**7c**) was synthesized using the same procedure. **7c**: Yield 68%. Anal. Calcd for $C_{14}H_{27}ClN_2PtSn$: C, 29.37; H, 4.75; N, 4.89. Found: C, 29.71; H, 4.63; N, 5.24.

[PtClMe$_2$(Me$_3$Sn)(paen-me$_2$)] (7d). To a stirred solution of [PtMe$_2$(paen-me$_2$)] (50.0 mg, 0.124 mmol) in benzene (3 mL) was added Me$_3$SnCl (124 mg, 0.621 mmol). The color of solution changed from purple to yellow. Hexane (10 mL) was added, and the resulting precipitate was isolated by filtration and washed with hexane. The off-white solid was dried *in vacuo*. Yield: 94%. Anal. Calcd for $C_{15}H_{30}ClN_3SnPt$: C, 29.95; H, 5.03; N, 6.98. Found: C, 30.28; H, 4.75; N, 6.90.

[PtBrMe$_2$(Me$_3$Sn)(py-*n*-pr)] (8b). To a stirred solution of [PtMe$_2$(py-*n*-pr)] (50.0 mg, 0.134 mmol) in toluene (5 mL) was added Me$_3$SnBr (75.0 mg, 0.308 mmol). An off-white precipitate formed within seconds. Hexane (10 mL) was added, and the solid was isolated by filtration and washed with hexane. Yield: 82%. Anal. Calcd for $C_{14}H_{27}BrN_2PtSn$: C, 27.25; H, 4.41; N, 4.54. Found: C, 27.57; H, 4.17; N, 4.50.

[PtBrMe$_2$(Me$_3$Sn)(paen-me$_2$)] (8c). To a stirred solution of [PtMe$_2$(paen-me$_2$)] (25.0 mg, 0.0621 mmol) in benzene (5 mL) was added Me$_3$SnBr (18.0 mg, 0.0740 mmol). A white precipitate formed almost immediately. Hexane (5 mL) was added, and the solid was isolated by filtration and washed with hexane. Yield: 91%. Anal. Calcd for $C_{15}H_{30}BrN_3PtSn$: C, 27.88; H, 4.68; N, 6.50. Found: C, 28.11; H, 4.50; N, 6.51.

[PtIMe$_2$(Me$_3$Sn)(py-*n*-pr)] (9b). To a stirred solution of [PtMe$_2$(py-*n*-pr)] (50.0 mg, 0.134 mmol) in toluene (5 mL) was added Me$_3$SnI (58 mg, 0.20 mmol). A yellow precipitate formed quickly. Hexane (10 mL) was added, and the solution was filtered off. The solid was washed with hexane and dried *in vacuo*. Yield: 79%. Anal. Calcd for $C_{14}H_{27}IN_2PtSn$: C, 25.32; H, 4.10; N, 4.22. Found: C, 25.47; H, 3.79; N, 4.10. [PtIMe$_2$(Me$_3$Sn)(paen-me$_2$)] (**9c**) was prepared as described for [PtIMe$_2$(Me$_3$Sn)(py-*n*-pr)]. **9c**: Yield 92%. Anal. Calcd for $C_{15}H_{30}IN_3PtSn$: C, 25.99; H, 4.36; N, 6.06. Found: C, 25.99; H, 4.20; N, 5.86.

[PtClMe$_2$(Me$_2$SnCl)(paen-me$_2$)] (10a). To a stirred solution of [PtMe$_2$(paen-me$_2$)] (101 mg, 0.250 mmol) in benzene (5 mL) was added Me$_2$SCl$_2$ (275 mg, 1.25 mmol). An off-white precipitate formed. Hexane (5 mL) was added, and the solid was isolated by filtration, washed with hexane, and dried *in vacuo*. Yield: 92%. Anal. Calcd for $C_{14}H_{27}Cl_2N_3SnPt$: C, 27.03; H, 4.37; N, 6.75. Found: C, 26.95; H, 4.20; N, 6.57.

[PtClMe$_2$(Me$_2$SnCl)(bpy-^{t}bu$_2$)] (10b). To a stirred suspension of [PtMe$_2$(bpy-^{t}bu$_2$)] (0.600 g, 1.22 mmol) in toluene (5 mL) was added Me$_2$SnCl$_2$ (1.34 g, 6.10 mmol). The solution turned yellow, and an off-white precipitate formed after 1 min. The solid was isolated by filtration, washed with toluene and pentane, and dried *in vacuo*. Yield: 92%. Anal. Calcd for $C_{22}H_{36}Cl_2N_2PtSn$: C, 37.05; N, 5.09; N, 3.93. Found: C, 36.78; H, 5.02; N, 3.71. [PtClMe$_2$(MeSnCl$_2$)(paen-me$_2$)] (**11**) and [PtBrMe$_2$(Me$_2$SnBr)(bpy-^{t}bu$_2$)]·0.5Me$_2$SnBr$_2$ (**B**) were synthesized by the same procedure except 1.1 equiv of MeSnCl$_3$ was used in the synthesis of **11**. **11**: Yield 97%. Anal. Calcd for $C_{13}H_{24}Cl_3N_3PtSn$: C, 24.30; H, 3.77; N, 6.54. Found: C, 24.43; H, 3.87; N, 6.53. **B**: Yield 97%. Anal. Calcd for $C_{23}H_{39}Br_3N_2PtSn_{1.5}$: C, 28.89; H, 4.11; N, 2.93. Found: C, 29.02; H, 4.07; N, 2.92.

[PtClMe$_2$(SnCl$_3$)(paen-me$_2$)] (12). To a solution of [PtMe$_2$(paen-me$_2$)] (50.0 mg, 0.124 mmol) in CH$_2$Cl$_2$ (1 mL) at −78 °C was added SnCl$_4$ (130 μL, 1.30 mmol). The solution was allowed to warm to room temperature. A bright-yellow solid formed, and this was isolated by filtration and dried *in vacuo*. Yield: 94%. Anal. Calcd for $C_{12}H_{21}C_{14}N_3PtSn$: C, 21.74; H, 3.19; N, 6.34. Found: C, 22.08; H, 3.38; N, 5.80.

[PtClMe$_2$(Me$_3$Ge)(bpy-^{t}bu$_2$)] (13). To a solution of [PtMe$_2$(bpy-^{t}bu$_2$)] (93.0 mg, 0.188 mmol) in CH$_2$Cl$_2$ (1 mL) was added Me$_3$GeCl (173 mg, 1.13 mmol). The solution changed from orange to yellow, and hexane (5 mL) was added to precipitate the product. A yellow solid was isolated and dried in vacuo. Yield: 89%. Anal. Calcd for $C_{23}H_{39}ClGeN_2Pt$: C, 42.72; H, 6.08; N, 4.33. Found: C, 42.30; H, 5.73; N, 4.11. [PtBrMe$_2$(Me$_3$Ge)(bpy-^{t}bu$_2$)] (**14**), [PtIMe$_2$(Me$_3$Ge)(bpy-^{t}bu$_2$)] (**15**), and [PtBrMe$_2$(Me$_3$Si)(bpy-^{t}bu$_2$)] (**19b**) were synthesized by the same procedure described for [PtClMe$_2$(Me$_3$Ge)(bpy-^{t}bu$_2$)] except that 2 equiv of Me$_3$GeBr, 1.1 equiv of Me$_3$GeI, and 5 equiv of Me$_3$SiBr were used in each reaction, respectively. **14**: Yield 54%. Anal. Calcd for $C_{23}H_{39}BrGeN_2Pt$: C, 39.97; H, 5.69; N, 4.05. Found: C, 39.57; H, 5.72; N, 4.10. **15**: Yield 85%. Anal. Calcd for $C_{23}H_{39}GeIN_2Pt$: C, 37.43; H, 5.33; N, 3.80. Found: C, 37.58; H, 4.48; N, 4.00. **19b**: Yield 84%. Anal. Calcd for $C_{23}H_{39}BrN_2PtSi$: C, 42.72; H, 6.08; N, 4.33. Found: C, 42.48; H, 5.81; N, 4.23.

[PtClMe$_2$(Me$_3$Sn)(bpy-^{t}bu$_2$)]·Me$_3$SnCl (16). To a suspension of [PtMe$_2$(bpy-^{t}bu$_2$)] (0.300 g, 0.608 mmol) in toluene (10 mL) was added Me$_3$SnCl (0.605 mg, 3.04 mmol). The resulting off-white suspension was filtered out and washed with hexane. Yield: 93%. Anal. Calcd for $C_{26}H_{48}Cl_2N_2Sn_2Pt$: C, 35.01; H, 5.42; N, 3.14. Found: C, 35.07; H, 4.86; N, 3.19.

[PtBrMe$_2$(Me$_3$Sn)(bpy-^{t}bu$_2$)]·Me$_3$SnBr (17). To a stirred suspension of [PtMe$_2$(bpy-^{t}bu$_2$)] (50.0 mg, 0.101 mmol) in toluene (10 mL) was added Me$_3$SnBr (124 mg, 0.507 mmol). An off-white precipitate was formed, and the solution was stirred for 10 min after which time 10 mL of pentane was added. The solid was isolated by filtration, washed with pentane, and dried *in vacuo*. Yield: 96%. Anal. Calcd for $C_{26}H_{48}Br_2N_2PtSn_2$: C, 31.84; H, 4.93; N, 2.86. Found: C,

---

(49) McWilliam, D. C.; Wells, P. R. *J. Organomet. Chem.* **1975**, *85*, 165.

(50) Lesbre, M.; Mazerolles, P. *Compt. Rend.* **1958**, 1708.

32.00; H, 4.86; N, 2.83. [PtIMe$_2$(Me$_3$Sn)(bpy-^{t}bu$_2$)]·Me$_3$SnI (**18**) was synthesized by the same procedure. **18**: The yield of yellow solid was 67%. Anal. Calcd for $C_{26}H_{48}I_2N_2PtSn_2$: C, 29.05; H, 4.50; N, 2.61. Found: C, 30.82; H, 4.61; N, 2.92.

[PtBrMe$_2$(Me$_3$Si)(py-*n*-pr)] (19c). To a stirred solution of [PtMe$_2$(py-*n*-pr)] (75.0 mg, 0.200 mmol) in toluene (3 mL) was added 5 equiv of Me$_3$SiBr (154 mg, 1.00 mmol). The solution remained red after 10 min. CH$_2$Cl$_2$ (2 mL) was then added, and the solution was stirred for a further 1 h. The solvent volume was reduced to 2 mL, resulting in a red solution and an off-white solid. The solid was isolated and washed with hexane. Yield: 50%. Anal. Calcd for $C_{14}H_{27}BrN_2PtSi$: C, 31.94; H, 5.17; N, 5.32. Found: C, 31.96; H, 4.59; N, 5.07.

[PtBrMe$_2$(Me$_3$Si)(paen-me$_2$)] (19d). To a stirred suspension of [PtMe$_2$(paen-me$_2$)] (100 mg, 0.249 mmol) in benzene (2 mL) was added Me$_3$SiBr (232 mg, 1.52 mmol). After 2 h, an off-white precipitate was evident. The solid was isolated by filtration, washed with benzene and then hexane, and dried *in vacuo*. Yield: 83%. Anal. Calcd for $C_{15}H_{30}BrN_3PtSi$: C, 32.20; H, 5.40; N, 7.15. Found: C, 32.22; H, 5.12; N, 7.53.

[PtIMe$_2$(Me$_3$Si)(bpy-^{t}bu$_2$)] (20b). To a stirred suspension of [PtMe$_2$(bpy-^{t}bu$_2$)] (50.0 mg, 0.101 mmol) in toluene (5 mL) was added Me$_3$SiI (101 mg, 0.507 mmol). To the bright yellow solution was added hexane (15 mL), and precipitation of a yellow microcrystalline solid occurred. The solution was filtered off, and the solid was washed with hexane and then dried *in vacuo*. Yield: 90%. Anal. Calcd for $C_{23}H_{39}IN_2PtSi$: C, 39.83; H, 5.67; N, 4.04. Found: C, 40.13; H, 5.65; N, 4.28.

[PtIMe$_2$(Me$_3$Si)(py-*n*-pr)] (20c). To a stirred solution of [PtMe$_2$(py-*n*-pr)] (75.0 mg, 0.200 mmol) in toluene (2 mL) was added Me$_3$SiI (140 mg, 0.700 mmol). Within 3 min, a bright-yellow precipitate had formed. The solid was isolated by filtration and washed with hexane. Yield: 82% Anal. Calcd for $C_{14}H_{27}IN_2PtSi$: C, 29.32; H, 4.75; N, 4.88. Found: C, 29.12; H, 4.33; N, 4.82.

[PtIMe$_2$(Me$_3$Si)(paen-me$_2$)] (20d). To a solution of [PtMe$_2$(paen-me$_2$)] (50.0 mg, 0.124 mmol) in toluene (5 mL) was added Me$_5$SiI (124 mg, 0.621 mmol). A yellow precipitate formed immediately. Hexane (5 mL) was added, and the solid was isolated by filtration and washed with toluene and hexane. Yield: 80%. Anal. Calcd for $C_{15}H_{30}IN_3PtSi$: C, 29.90; H, 5.02; N, 6.97. Found: C, 30.04; H, 4.79; N, 7.19.

[PtIMe$_2$(Me$_3$Sn)(bpy-^{t}bu$_2$)]$_2$·Me$_3$SnI·CH$_2$Cl$_2$ (A). [PtIMe$_2$(Me$_3$Sn)(bpy-^{t}bu$_2$)]·Me$_3$SnI (50 mg, 0.046 mmol) was dissolved in CH$_2$Cl$_2$ (2 mL), and Me$_3$SnI (27 mg, 0.093 mmol) was added. The solution was filtered into a 7 mm crystallization tube and cooled to −30 °C. Room-temperature CH$_2$Cl$_2$ (0.3 mL) was layered onto the cold CH$_2$Cl$_2$ solution, and pentane (5 mL) was then layered onto the CH$_2$Cl$_2$. The tube was capped and kept at −30 °C in the refrigerator of a drylab. After 3 weeks, yellow crystals suitable for X-ray crystallographic study had formed. The solvent was poured out of the tube, and the remaining solvent was allowed to evaporate at room temperature from the inverted tube. X-ray crystallographic study indicated the above formula.

Additions of Si−Cl Bonds to Platinum(II). Addition of 10−100-fold excesses of Me$_n$SiCl$_{4-n}$ (n = 1−3) to solutions of [PtMe$_2$(bpy-^{t}bu$_2$)] in toluene or CH$_2$Cl$_2$ did not result in any observed reaction, even after 48 h.

Additions of Group 14−Halogen Bonds to [PtXMe(bpy-^{t}bu$_2$)] (X = Br, I). Addition of 10-fold excesses of Me$_3$EBr (E = Si, Sn) to a solution of [PtBrMe(bpy-^{t}bu$_2$)] (30.0 mg, 0.0537 mmol) in CH$_2$Cl$_2$ (1 mL) did not result in any observable reaction after 1 h. No reactions were observed for the addition of Me$_3$EI (E = Si, Sn) to [PtIMe(bpy-^{t}bu$_2$)].

X-ray Structure Determinations. Yellow crystals of [PtIMe$_2$(Me$_3$Si)(bipy)] (**20a**) were obtained by the diffusion of *n*-pentane into a CH$_2$Cl$_2$ solution of the compound at −30 °C. A crystal of suitable size (0.12 × 0.12 × 0.18 mm) was obtained by cutting a long rodlike crystal along the (110) plane. Light-yellow needles of [PtIMe$_2$(Me$_3$Sn)(bipy-^{t}bu$_2$)]·0.5Me$_3$SnI·CH$_2$Cl$_2$ (**A**) were grown using the same method as for **20a**. The crystals were found to loss the dichloromethane solvent slowly in air and became opaque at room temperature. Crystals of suitable size (0.16 × 0.16 × 0.16 mm) were obtained by cutting a long plates and were wedged inside Lindemann capillary tubes and flame sealed. The crystallographic data for the two crystals are presented in Table 5.

Table 5. Crystallographic Details for the Structures

	20a	A
formula	$C_{15}H_{23}N_2I_1Pt_1Si_1$	$C_{50}H_{89}Cl_2I_3N_4Pt_2Sn_3$
fw	581.427	1944.18
T, K	291	299
λ, Å	0.710 73	0.710 73
space group	$P2_1/n$	$P2_1/m$
a, Å	14.371(2)	11.204(2)
b, Å	9.371(2)	13.926(2)
c, Å	13.865(2)	22.485(3)
β, deg	90.99(1)	96.40(1)
V, Å^3	1867(1)	3486.5(9)
Z	4	2
ρ_{calcd}, g cm^{-3}	2.08	1.85
ρ_{obs}, g cm^{-3}	2.08(2)	1.87(5)
μ, mm^{-1}	9.288	6.47
F(000)	1087.72	1832
NO[a]	2272 [$\mathbf{I} \geq 2.5\sigma(\mathbf{I})$]	2250 [$F > 4.0\sigma(F)$]
R[b]	0.040	0.0676
R_w[c]	0.051	0.0681
S[d]	1.21	1.33

[a] NO = number of observed reflections. [b] $R = \sum(||F_o| - |F_c||)/\sum|F_o|$. [c] For **20a**, $R_w = [\sum w(|F_o| - |F_c|)^2/(\sum wF_o^2)]^{1/2}$; for **A**, $R_w = [\sum w(|F_o| - |F_c|)w/^{1/2}/(\sum w|\sum F_o^2)]^{1/2}$. [d] S = goodness of fit; $S = [\sum w(|F_o| - |F_c|)^2/(M - N)]^{1/2}$, where M is the number of reflections and N is the number of parameters refined.

20a. The data collection was carried out on an Enraf-Nonius CAD4F diffractometer using graphite-monochromated Mo Kα radiation[51] at 18 °C. Photo and automatic indexing routines, followed by least-squares fits of 21 accurately centered reflections (24.1 ≤ 2θ ≤ 31.6°), gave cell constants and an orientation matrix. The Niggli matrix and an observation of symmetry equivalent data suggested the monoclinic system and Laue symmetry 2/*m*, respectively. Intensity data were recorded in the ω mode, at variable scan speeds (1.37−4.12 deg min^{-1}) and a scan width of 0.80 + 0.35 tan θ, with a maximum time per datum of 60 s. Background measurements were made by extending the scan by 25% on each side. Three standard reflections were monitored every 180 min of X-ray exposure time. In all 3975 reflections in the 2θ range 0−50° ($-17 \leq h \leq 17$, $-11 \leq k \leq 1$, $-16 \leq l \leq 1$) and 25 repetitions of the standards were recorded. The NRCVAX crystal structure programs[52] running on a SUN 3/80 workstation were used for data processing and least-squares refinements. The data were corrected for Gaussian absorption (10 faces with face indices {101}, {110}, and {100}, μ = 9.288 mm^{-1}) and gave maximum and minimum transmission factors 0.474 and 0.367. The systematic absences suggested the space group $P2_1/n$. The equivalent reflections were averaged (R_{int} = 0.032) leaving 3277 independent reflections. The structure solution and the refinements were done by full-matrix least-squares techniques on F. The structure was solved by the SHELXS-86 program[53] and subsequent different Fourier techniques. Nine hydrogen atom positions were located in the difference Fourier, most of which were found near methyl carbon atoms. On the basis of these positions, the rest of the hydrogen atoms were placed in the calculated positions (C−H = 1.08 Å), and their thermal parameters were assigned 10% more of the attached carbon atoms before each least-squares cycles. Anisotropic thermal parameters were assigned for all non-hydrogen atoms and

---

(51) *CAD4 Diffractometer Manual*; Enraf-Nonius: Delft, The Netherlands, 1988.

(52) Gabe, E. J.; Le Page, Y.; Charland, J.-P.; Lee, F. C. *J. Appl. Crystallogr.* **1989**, *22*, 384.

(53) Sheldrick, G. M. *Acta Crystallogr.* **1990**, *A46*, 467.

were refined. In the final cycles, the refinement of 181 parameters and 2272 ($I \geq 2.5\sigma(I)$) observations gave a convergent model at $R = 0.040$, $R_w = 0.051$, and $S = 1.21$ using the weighting scheme based on counting statistics with weighted modifier K in $KF_o^2 = 0.001$. The final difference Fourier synthesis had four peaks with electron density in the range 2.66−1.22 e Å^{-3} which were associated with Pt and I atoms at distances of 1.03−1.09 Å. All other peaks had electron density below 0.66 e Å^{-3}. A relatively large residual electron density around the heavy atoms may be attributed to poorer absorption correction due to cut faces. The largest $\Delta/\sigma = 0.059$. Atomic coordinates and B_{iso} values are available in the Supporting Information.

A. Light-yellow needles were grown by diffusion of *n*-pentane into a CH_2Cl_2 solution of complex at −30 °C. ^1H NMR spectroscopy indicated both free Me_3SnI and CH_2Cl_2 to be present in a solution of the crystals obtained. The density of the crystal was determined by the neutral buoyancy method using a mixture of carbon tetrachloride and dibromomethane. The diffraction experiments were carried out on a Siemens P4 4-circle diffractometer with XSCANS software package[54] using graphite-monochromated Mo Kα radiation at 26 °C. The cell constants were obtained by centering 28 high-angle reflections ($24.2 \leq 2\theta \leq 24.9°$). The Laue symmetry $2/m$ was determined by merging symmetry-equivalent reflections. During data collection three standards were monitored for every 197 data measured. In total 5556 reflections were collected in the 2θ range 3.5−45° ($-12 \leq h \leq 1$, $-14 \leq k \leq 1$, $-24 \leq l \leq 24$) in $\theta-2\theta$ scan mode at variable scan speeds (2−10 deg/min). Background measurements were made at the ends of the scan range. The data processing, solution, and the refinements were done using SHELXTL-PC programs.[55] The data were corrected for absorption ($\mu = 6.47$ mm^{-1}) by an empirical method involving ψ scans techniques using 15 reflections ($7.3 < 2\theta < 22.4°$). The maximum and minimum transmission factors were 0.102 and 0.071, respectively ($R_{int} = 4.4\%$). For a primitive cell, the systematic absences ($0k0$, $k = 2n + 1$) suggest two possible space groups, $P2_1$ (No. 4) or $P2_1/m$ (No. 11). The mean $e^2 - 1$, 0.891, suggested a noncentrosymmetric space group (expected 0.968 for centrosymmetric and 0.736 for noncentrosymmetric). For $Z = 2$, the space group $P2_1$ was chosen first and the structure was solved. The program MISSYM[56] suggested an extra mirror plane in the molecule disregarding the hydrogen atoms and the disordered methyl carbon atoms. Therefore, the structure was again solved in the space $P2_1/m$ and successfully refined. The atoms Pt(1), Sn(1), I(1), Pt(2), Sn(2), I(2), Sn(3), and I(3) and the methyl carbon atoms C(11) and C(31) were found to be sitting on the mirror plane. Anisotropic thermal parameters were assigned and refined for the Pt, Sn, and I atoms. At this stage, the isotropic thermal parameters for the methyl groups C(11), C(12), C(28), C(29), and C(30) were high, indicating the possibility of disorder. Two disorder models were found for the methyl groups attached to the C(27) atom with occupancies 0.55 and 0.45. These two models (C(28)−C(30) and C(28′)−C(30′)) were refined with a restrained ideal geometry; i.e., common C−C and C⋯C (1.633 times C−C length) distances were assigned and refined for all these methyl carbon atoms. Common isotropic thermal parameters were assigned for each disorder group and refined in the least-squares cycles. The methyl group disorders around tin in the Me_3SnI fragment were also successfully resolved. Of the three different orientations of the methyl groups, two were related by the presence of a mirror (i.e. one set of methyl groups (C(33), C(34), and C(35)) produces the other disorder fragment by mirror symmetry). In the third model, C(36) sits on the mirror and C(37) is present in the general position. Common Sn−C and C⋯C (1.732 times Sn−C length) distances were assigned for all these three models and refined in the least-squares cycles. The occupancy factors deduced by comparing the electron densities obtained from the difference Fourier peaks were 0.333 and 0.333 for these fragments. The disorder associated with C(11) and C(12) could not be resolved due to smearing of electron density as indicated by the electron density maps, and a disordered model using rigid groups could not be formulated. In one attempt both these carbon atoms were assigned anisotropic thermal parameters and refined in the least-squares cycles. Since the isotropic equivalent displacement parameters (Å^2) were unreasonably high ($U_{eq} = 0.49(2)$), the isotropic thermal parameter was fixed ($U = 0.15$) for C(12) and not refined in the subsequent least-squares cycles. All the hydrogen atoms except those bonded to the disordered carbon atoms were placed in the calculated positions, and they were included for the purpose of structure factor calculations only. A common thermal parameter was assigned for these hydrogen atoms and refined in the least-squares cycles. There was some leftover electron density which was recognized as CH_2Cl_2 with the support of ^1H NMR spectroscopic data. This solvent molecule was found to be severely disordered near the mirror plane. The disorder was satisfactorily resolved. Rigid group restraints were applied (C−Cl = 1.65 Å and Cl⋯Cl = 2.694 Å) in the least-squares cycles. A common isotropic thermal parameter was assigned for each disorder model and refined in the least-squares cycles. In the final least-squares refinement cycles, the model converged at $R = 6.76\%$, $wR = 6.81\%$, and $S = 1.33$ for 2250 observations with $F_o \geq 4\sigma(F_o)$ and 236 parameters. The largest and mean Δ/σ values were 0.072 and 0.003, respectively. The electron density in the final difference Fourier synthesis fluctuates between 1.06 and −1.25 e Å^{-3}. The top two peaks were near Sn(1) and Pt(2) at distances 0.95 and 1.03 Å, respectively. The isotropic extinction parameter was refined to $5(1) \times 10^{-5}$. Atomic coordinates and U_{eq} values are in the Supporting Information.

Acknowledgment. We thank the Natural Sciences and Engineering Council of Canada for financial support to R.J.P. and a postgraduate scholarship to C.J.L. We also thank N. C. Payne for use of the crystallographic facilities.

Supporting Information Available: Text giving full ^1H NMR parameters and tables listing full details on the X-ray structure determinations for $[PtIMe_2(Me_3Si)(bipy)]$ and $[PtIMe_2(Me_3Sn)(bipy\text{-}^tbu_2)]_2 \cdot Me_3SnI \cdot CH_2Cl_2$ (22 pages). Ordering information is given on any current masthead page.

OM950493U

---

[54] *XSCANS*; Siemens Analytical X-Ray Instruments Inc.: Madison, WI, 1990.

[55] Sheldrick, G. M. *SHELXTL-PC Software*; Siemens Analytical X-Ray Instruments Inc.: Madison, WI, 1990.

[56] Le Page, Y. *J. Appl. Crystallogr.* **1987**, *20*, 264.